

Towards Realistic Understandings of Gas Dynamics in Protoplanetary Disks

Xue-Ning Bai

Institute for Advanced Study and Center for Astrophysics, Tsinghua University
Beijing 100084, China
email: xbai@tsinghua.edu.cn

Abstract. The gas dynamics of protoplanetary disks (PPDs) plays a crucial role in almost all stages of planet formation, yet it is far from being well understood largely due to the complex interplay among various microphysical processes. Primarily, PPD gas dynamics is likely governed by magnetic fields, and their coupling with the weakly ionized gas is described by non-ideal magnetohydrodynamic (MHD) effects. Incorporating these effects, I will present the first fully global simulations of PPDs that include the most realistic disk microphysics. Accretion and disk evolution is primarily driven by magnetized disk winds with significant mass loss comparable to accretion rate. The overall disk gas dynamics strongly depends on the polarity of large-scale poloidal magnetic field threading the disk owing to the Hall effect. The flow structure in the disk is highly unconventional with major implications on planet formation.

Keywords. accretion disks, MHD, planetary systems: protoplanetary disks

1. Introduction

The gas dynamics of protoplanetary disks (PPDs) is primarily governed by the mechanism that drives angular momentum transport (AMT). This is observationally linked to the typical accretion rate of the order $10^{-8}M_{\odot} \text{ yr}^{-1}$ (Hartmann *et al.* 1998), as well as outflows that are ubiquitously found from young stellar objects (Hartigan *et al.* 1995, Simon *et al.* 2016). Conventionally, AMT in PPDs is thought to be mediated by turbulence driven by the magnetorotational instability (MRI, Balbus & Hawley 1991, Gammie 1996), which transports angular momentum radially outward. Alternatively, angular momentum can be transported vertically via a magnetized disk wind (Blandford & Payne 1982), which requires a large-scale poloidal field threading the disk.

Both the MRI and disk wind scenarios are sensitive to the level of coupling between gas and magnetic field in the disk, which is tied to the level of ionization. The PPDs largely rely on external sources of non-thermal ionization (except for the innermost region where alkali species can be thermally ionized). These include stellar X-rays, far-UV (FUV), and cosmic-rays, which all have finite penetration depth and only ionize the disk very weakly. They also contribute to substantial heating at the disk surface.

Magnetic fields are no longer frozen in to weakly ionized gas, which is described by non-ideal magnetohydrodynamic (MHD) effects. They are reflected to the induction equation, which describes how magnetic fields evolve (valid in the absence of charged grains):

$$\frac{\partial \mathbf{B}}{\partial t} = \nabla \times (\mathbf{v} \times \mathbf{B}) + \nabla \times \left[\frac{4\pi\eta}{c} \mathbf{J} + \frac{\mathbf{J} \times \mathbf{B}}{en_e} - \frac{(\mathbf{J} \times \mathbf{B}) \times \mathbf{B}}{c\gamma\rho\rho_i} \right]. \quad (1.1)$$

In the above, $\mathbf{J} = c\nabla \times \mathbf{B}/4\pi$ is the current density, ρ , ρ_i are the densities of gas and ions, n_e is the electron number density, γ is the coefficient of momentum transfer between ions and neutrals, $\eta \propto 1/n_e$ is the resistivity. The last three terms on the right hand side

correspond to Ohmic resistivity (O), the Hall effect (H), and ambipolar diffusion (A). In terms of their strength, they are all inversely proportional to the ionization fraction ($1/n_e$). In the mean time, the relative importance of the three terms is determined by gas density and field strength, with $\eta_O \propto (B/\rho)^0$, $\eta_H \propto (B/\rho)^1$, and $\eta_A \propto (B/\rho)^2$.

Applied to PPDs, it turns out that resistivity is important only in the densest part of the disk, namely, the midplane region of the inner disk (with $R \lesssim 5 - 10$ AU). Moving towards the surface, as density drops, we transition first to the Hall-dominated regime, followed by ambipolar diffusion dominated region (e.g., Wardle 2007, Bai 2011). In the very upper layer, FUV substantially boosts the ionization fraction, and the gas behaves close to ideal MHD Perez-Becker & Chiang 2011).

The role of resistivity has been extensively studied in the literature (e.g., Fleming & Stone 2003, Fleming & Stone 2003, Ilgner & Nelson 2006, Bai & Goodman 2009), giving the picture of layered accretion where the MRI is suppressed in the Ohmic-dominated midplane region of inner disk, while remain active in the surface layer. This picture has been challenged once the other two non-ideal MHD effects are taken into account: it has been found that in the surface layer of the inner disk, ambipolar diffusion is sufficiently strong that can fully suppress the MRI, and hence disk accretion must be driven by a magnetized disk wind (Bai & Stone 2013, Gressel *et al.* 2015). This means that a large-scale poloidal field threading the disk is essential, which is likely inherited from the star formation process.

In addition, in the presence of background poloidal field, the Hall effect makes the dynamics depend on the polarity of this field, which can be seen from Equation (1.1): the equation remains valid by changing the sign of \mathbf{B} except for the Hall term. We call the case with $\mathbf{B} \cdot \boldsymbol{\Omega} > 0$ the “aligned” case, and $\mathbf{B} \cdot \boldsymbol{\Omega} < 0$ for “anti-aligned” case. The role of the Hall term has been studied in terms of local shearing-box simulations (e.g., Lesur *et al.* 2014, Bai 2014). Besides certain ambiguities inherited to local simulations, it has been found that the aligned case leads to the Hall-shear instability (HSI, Kunz 2008), which strongly amplifies the horizontal component of the magnetic field, whereas in the anti-aligned case, growth horizontal field is suppressed.

Previous works have largely been conducted using local simulations (aforementioned), or semi-global simulations with truncated vertical/latitudinal boundaries (e.g., Gressel *et al.* 2015, Béthune *et al.* 2017). While they clearly demonstrate wind launching, wind kinematics can not be properly determined due to artificial truncation of the vertical boundary. Moreover, many of these simulations are subject to symmetry issues. It is thus highly desirable to conduct fully global disk simulations with fully covered simulation domain to accommodate wind launching, together with well-resolved disk microphysics.

2. Simulations and Results

In this work, using the Athena++ MHD code (Stone *et al.* in prep), we present the first set of such simulations to date for the inner region ($\sim 1 - 20$ AU) of PPDs. Since we expect the MRI to be suppressed in this region, our simulations are conducted in 2D in spherical polar coordinates. We set up a thin disk with prescribed surface density profiles $\Sigma = 500 R_{\text{AU}}^{-1} \text{g cm}^{-2}$ as well as temperature profiles in hydrostatic equilibrium. The temperature is set so that disk aspect ratio $\epsilon \sim 0.05 - 0.1$ in the midplane and increases to $\epsilon = 0.2$ at the atmosphere (to mimic external heating), maintained by a simple cooling prescription. Radial ray tracing is done to track FUV (assumed penetration depth $\Sigma_{\text{FUV}} = 0.03 \text{g cm}^{-2}$), as well as X-ray and cosmic-ray ionizations with standard prescriptions. All three non-ideal MHD effects are included, with diffusivities interpolated from a pre-computed lookup table. The radial grid to span from $r_{\text{in}} = 0.6$ AU to $r_{\text{out}} = 60$ AU with logarithmic grid spacing. The θ -grid extends from the midplane all the way to

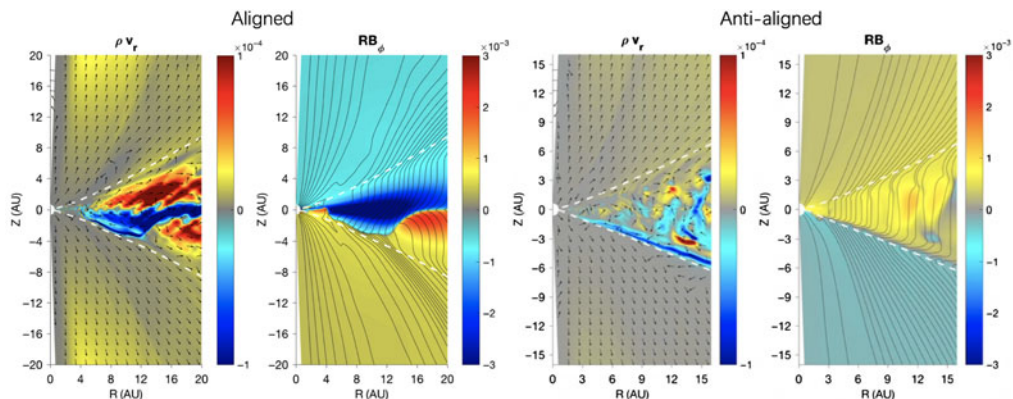


Figure 1. Last snapshot of the fiducial simulation runs. Left/right two panels are for aligned and anti-aligned cases. In each group, the left figure shows the radial mass flux ρv_r (color), with arrows indicating poloidal velocity directions (unit vectors). The right figure shows the magnetic field configurations (color represents B_ϕ , lines indicate poloidal field lines). White dashed lines mark the FUV front. Color bars are in dimensionless code units.

near the poles, and is concentrated around the disk which guarantees adequate resolution. The full grid size is 1152×512 in (r, θ) , and we achieve a grid resolution of about 15 – 20 cells per disk scale height. Poloidal fields are applied to the disks with initial plasma β_0 (ratio of gas to magnetic pressure) at the midplane to be 10^5 . The simulations are evolved to 1600 – 1800 yrs. More details are described in Bai (2017).

Figure 1 shows the magnetic field configurations and mass fluxes for simulations with aligned and anti-aligned field polarities at the end of the simulations. Wind launching are obvious in both cases, which we have found significant mass loss comparable or even in excess of the wind-driven accretion rates. Below we focus on the internal disk dynamics.

For the aligned case, the horizontal field strength is strongly amplified by the HSI. This is most intense in the inner few AU where the Hall effect is the strongest, making B_ϕ of a single sign dominating the entire disk vertical extent, before it flips at the very surface on one side to achieve a physical geometry for wind launching (i.e., to bend radially outward). Towards the outer region ($\gtrsim 10$ AU), as the Hall effect weakens, this flip occurs at the midplane, with a smooth transition. This is directly related to the radial mass flux, which can be shown to be approximately determined by $\rho v_R \approx B_z / (2\pi\Omega) \cdot (\partial B_\phi / \partial z)$. Correspondingly, we see that in the inner few AU, the gas flows inwards and outwards in either half of the disk midplane, plus additional accretion flow at the disk surface where B_ϕ flips. Towards the outer disk, the accretion flow is concentrated at the midplane, with radial mass outflows at the disk upper layers.

For the anti-aligned case, the Hall effect first attempts to reduce horizontal field in the midplane regions towards zero. But this makes the system slightly unstable, eventually leading to symmetry breaking with B_ϕ of one sign dominating the bulk disk, though the field strength is much weaker than that in the aligned case. As a result, the accretion flow is entirely concentrated at the location where B_ϕ flips, with is located at the disk surface and roughly coincides with the location of the FUV front. We find that this accretion flow is supersonic, which makes wind launching from this layer more dynamic.

3. Discussion and Future Directions

The PPD simulations we have conducted so far are the most realistic to date. They demonstrate not only the importance of wind-driven accretion, but also the unusual flow structures in disks that can only be captured when all major disk microphysical effects are

properly included. Given that almost all stages of planet formation sensitively depends on disk gas dynamics, this opens up the avenue to explore planet formation under the realistic disk physics, such as grain growth and dust transport, planetesimal formation, pebble accretion, planet migration, etc. Future works should continue to improve upon the thermal physics (e.g., Wang, Bai & Goodman 2019), extend the simulation to three dimensions, and further explore the hot innermost region and the cold outer disk regions.

References

- Bai, X.-N. 2011, *ApJ*, 739, 50
 Bai, X.-N. 2014, *ApJ*, 791, 137
 Bai, X.-N. 2017, *ApJ*, 845, 75
 Bai, X.-N., & Goodman, J. 2009, *ApJ*, 701, 737
 Bai, X.-N., & Stone, J. M. 2011, *ApJ*, 736, 144
 Bai, X.-N., & Stone, J. M. 2013, *ApJ*, 769, 76
 Béthune, W., Lesur, G., & Ferreira, J. 2017, *A&A*, 600, A75
 Balbus, S. A., & Hawley, J. F. 1991, *ApJ*, 376, 214
 Blandford, R. D., & Payne, D. G. 1982, *MNRAS*, 199, 883
 Fleming, T., & Stone, J. M. 2003, *ApJ*, 585, 908
 Gammie, C. F. 1996, *ApJ*, 457, 355
 Gressel, O., Turner, N. J., Nelson, R. P., & McNally, C. P. 2015, *ApJ*, 801, 84
 Hartigan, P., Edwards, S., & Ghandour, L. 1995, *ApJ*, 452, 736
 Hartmann, L., Calvet, N., Gullbring, E., & D'Alessio, P. 1998, *ApJ*, 495, 385
 Ilgner, M., & Nelson, R. P. 2006, *A&A*, 445, 205
 Kunz, M. W. 2008, *MNRAS*, 385, 1494
 Lesur, G., Kunz, M. W., & Fromang, S. 2014, *A&A*, 566, A56
 Perez-Becker, D., & Chiang, E. 2011, *ApJ*, 735, 8
 Simon, M. N., Pascucci, I., Edwards, S., *et al.* 2016, *ApJ*, 831, 169
 Wang, L., Bai, X.-N., & Goodman, J. 2019, *ApJ*, 874, 90
 Wardle, M. 2007, *AP&SS*, 311, 35

Discussion

LINSKY: Do your calculations include heating in the inner disk produced by shearing of the stellar and disk magnetic fields leading to flaring? I think that magnetic reconnection and heating is essential for estimating the ionization in the inner disk.

BAI: I divide the disk into “innermost”, “inner”, and “outer” regions, where the innermost region (up to a fraction of AU) is the most complex with thermal ionization, dust sublimation, and magnetospheric interactions taking place over a narrow range of radii. This work has focussed on the inner disk (1-20 AU) where the physics is cleaner. Energetic processes in the innermost region generally do not directly impact inner/outer disks, and X-rays/UV from there are jointly incorporated as part of the stellar properties.

LONGMORE: Your simulations focussed on isolated disks, but we heard yesterday that many disks formed next to high mass stars, so sit in a very strong uv-radiation field, and presumably regions of enhanced x-ray and CR fluxes. How would your result change for disks sitting in such environments?

BAI: The simulations we have so far have primarily focussed on the inner disk with $R \sim 1 - 20$ AU, where influence from the host protostar plays the dominant role. Environmental influence is known to be sometimes important in the outer disk (~ 100 pc scale), which we are working to incorporate in future works.